# The Complex Thiol-Palladium Interface: a Theoretical and Experimental Study

*Pilar Carro[a]\*, Gastón Corthey[b], Aldo Rubert[b], Guillermo Benitez[b], Mariano H. Fonticelli[b] and Roberto C. Salvarezza[b],*

a) Departamento de Química Física, Universidad de La Laguna, Tenerife, Spain

b) Instituto de Investigaciones Fisicoquímicas Teóricas y Aplicadas (INIFTA), Universidad Nacional de La Plata - CONICET, Sucursal 4 Casilla de Correo 16 (1900) La Plata, Argentina

\*pcarro@ull.es

## 1. Pd Electrodeposition on Preferred Oriented Au(111) Substrates.

Pd electrodeposition on preferred oriented Au(111) substrates was made from 1 mM $PdCl_2$ + 2 mM HCl + 0.1 M $H_2SO_4$ aqueous solution.

For bulk Pd electrodeposition a potential ramp at 1 mV·s-1 from +0.80 V to -0.40 V was applied and the electrode was polarized at the negative potential limit (-0.40 V) for 10 min, i.e. in the overpotential deposition region (OPD). A typical cyclic voltammogram obtained for this system is shown in Figure S1 which is similar to those reported in literature.[1] The overall charge density deposited under these experimental conditions is equivalent to approximately 50 monolayers of Pd. Under these experimental conditions, Pd terraces with (111) preferred orientation were obtained as confirmed by STM.[2] There is also (111) texture in the bulk, which has been verified by powder X-ray diffraction measurements.[2]

For the deposition of approximately 1 Pd monolayer (ML) on Au(111), underpotential deposition (UPD) was employed. A potential ramp at 1 mV·s-1 from +0.80 V to approximately +0.52 V, just before the OPD of Pd starts, was applied and the electrode was taken out of the cell with the potential applied. With this method approximately 1 ML of Pd on Au(111) is obtained.[3] A typical cyclic voltammogram of this routine is shown in Figure S2. The real Pd coverage was measured by XPS.
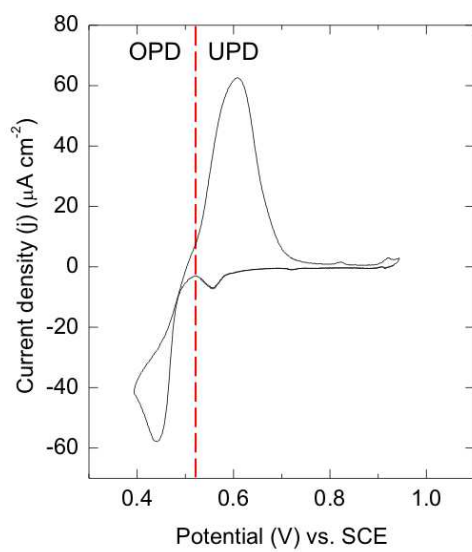
**Figure S1.** Typical cyclic voltammogram showing OPD Pd electrodeposition and dissolution processes on Au(111) from 1 mM PdCl$_2$ + 2 mM HCl + 0.1 M H$_2$SO$_4$ at 1 mV·s$^{-1}$.
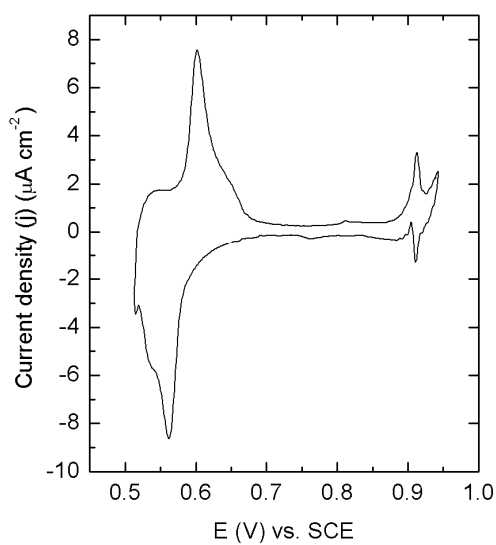


**Figure S2.** Typical cyclic voltammogram showing UPD Pd electrodeposition and dissolution processes on Au(111) from 1 mM PdCl$_2$ + 2 mM HCl + 0.1 M H$_2$SO$_4$ at 1 mV·s$^{-1}$.

## 2. X-ray Photoelectron Spectroscopy (XPS).

X-ray Photoelectron Spectroscopy (XPS) was performed using a Mg Kα source (XR50, Specs GmbH) and a hemispherical electron energy analyzer (PHOIBOS 100, Specs GmbH). A two point calibration of the energy scale was performed using sputtered cleaned gold (Au $4f_{7/2}$, binding energy (BE) = 84.00 eV) and copper (Cu $2p_{3/2}$, BE = 933.67 eV) samples. For spectra deconvolution of the S 2p region, a Shirley type background was subtracted and a combination of Lorentianz and Gaussian functions was used. The full width at half maximum (fwhm) was fixed at 1.1 eV and the spin-orbit doublet separation (SOS) of S 2p signal was set to 1.2 eV. The binding energies and peak areas were optimized to achieve the best adjustment.

Sulfide and thiolate coverage was estimated by the measurement of the areas of Pd 3d and S 2p signals corrected by the relative sensitivity factor (RSF) of the elements. In the case of bulk palladium, Pd 3d signal was corrected by the attenuation length for 3d electrons in palladium to consider only the signal of the top palladium atomic monolayer. Therefore, sulfide or thiolate coverage ($\theta_S$, $\theta_{thiol}$) is the ratio of S atoms to Pd atoms in the surface.

In the case of 1 Pd ML deposited on Au(111), the Pd coverage was estimated by the measurement of the areas of Pd 3d and Au 4d, by a deconvolution of that spectrum zone. For Pd 3d peaks a SOS of 5.25 eV was set, and the fwhm and BE positions as well as the Gaussian-Lorensian percentage were optimized for the best fit. The Au 4d signal was adjusted fixing the SOS to 18.1 eV with the other parameters allowed to fluctuate for the best fit. Then, the Pd coverage was calculated as the ratio of Pd 3d to Au 4d areas, taking into account the RSF and attenuation length for 3d electrons in Au.

## 3. Calculation of the standard chemical potential

Statistical thermodynamics has been applied in order to estimate the dimethyl disulfide standard chemical potential, $\mu^{\circ}_{(CH3S)_2}(T, p^{\circ})_{GAS}$ in terms of the molecular partition function.[41] Therefore, starting from

$$\mu^{\circ}_{(CH3S)_2}(T, p^{\circ})_{GAS} = -k_B T \ln\left[\left(\frac{q}{V}\right)\frac{k_B T}{p^0}\right]$$

and taking into account each contribution to the molecular partition function $q = q_t q_r q_v q_{elec}$ ($q_{elec}=1$), then:

$$\frac{q}{V} = \left[\left(\frac{2\pi m k_B T}{h^2}\right)^{3/2}\right]\left[\frac{\sqrt{\pi}T^{3/2}}{\sigma(\Theta_x \Theta_y \Theta_z)^{1/2}}\right]\left[\prod_i \frac{1}{1-e^{-v_i/k_B T}}\right]$$

where $m$ represents the molecular mass, $V$ the volume, $\sigma$ the symmetry number (equals 2) and $\Theta_{x,y,z}$ the rotational temperatures (in K) obtained from DFT calculation (Table S1).

In addition, the chemical potential, $\mu^{\circ}_{(CH_3S)_2}(T, p^0)_{LIG}$, for data related to adsorption from solution was calculated from the formation enthalpies $(\Delta_f H^{\circ})$ of the liquid and the gas phases[5] as well as the entropy change between the liquid and ideal gas state (Table 1).[6]

$$\mu^{\circ}_{(CH3S)_2}(T, p^0)_{LIQ} \cong \mu^{\circ}_{(CH3S)_2}(T, p^0)_{GAS} - \left[\left(\Delta_f H^{\circ}_{LIQ} - \Delta_f H^{\circ}_{GAS}\right) - T\left(S_{LIQ} - S_{GAS}\right)\right]$$

Therefore, the chemical potential of dimethyl disulfide in a solution with a given concentration ($c$) can be calculated by the following equation:

$$\Delta\mu(T, c_{(CH_3S)_2})_{LIQ} = \mu^{\circ}_{(CH_3S)_2}(T, p^0)_{LIQ} + k_B T \ln(c_{(CH_3S)_2})$$

**Table S1.** Parameters for the calculation of the standard chemical potential.

| | |
|---|---|
| $E^{ZPE}$ /eV | 2.15 |
| $\Theta_x$/K | 0.53683 |
| $\Theta y$/K | 0.12641 |
| $\Theta z$/K | 0.10519 |
| $\mu^0_{(CH_3S)_2}\left(T, p^0\right)_{GAS}$/eV | -0.813 |
| $\mu^0_{(CH_3S)_2}\left(T, p^0\right)_{LIQ}$/eV | -0.532 |

## 4. Initial geometry for models 4 and 5
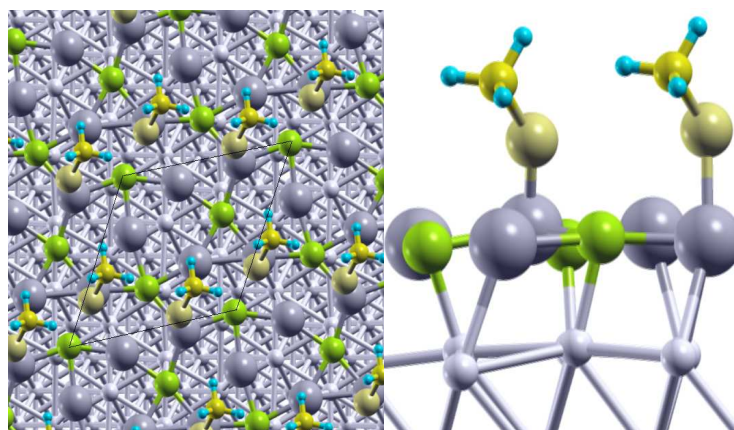


**Figure S3.** Initial model constructed which final relaxed structure resulted in model **4**.
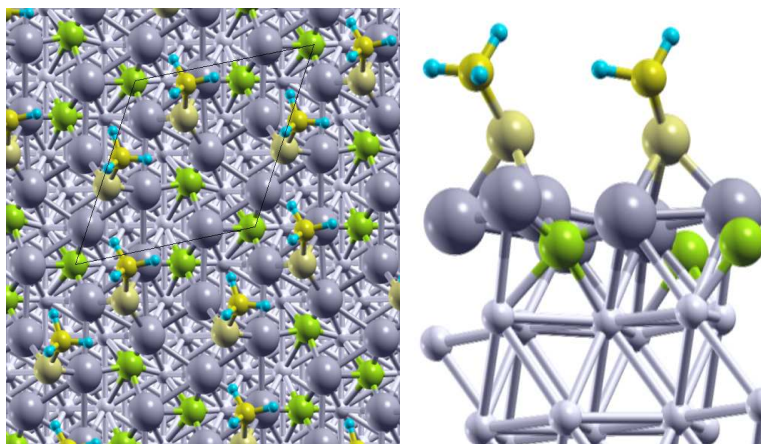
**Figure S4.** Initial model constructed which final relaxed structure resulted in model 5.

## 5. Structural parameters of the optimized models 4, 5, and thiol adatom models on Au(111).



(a)



(b)
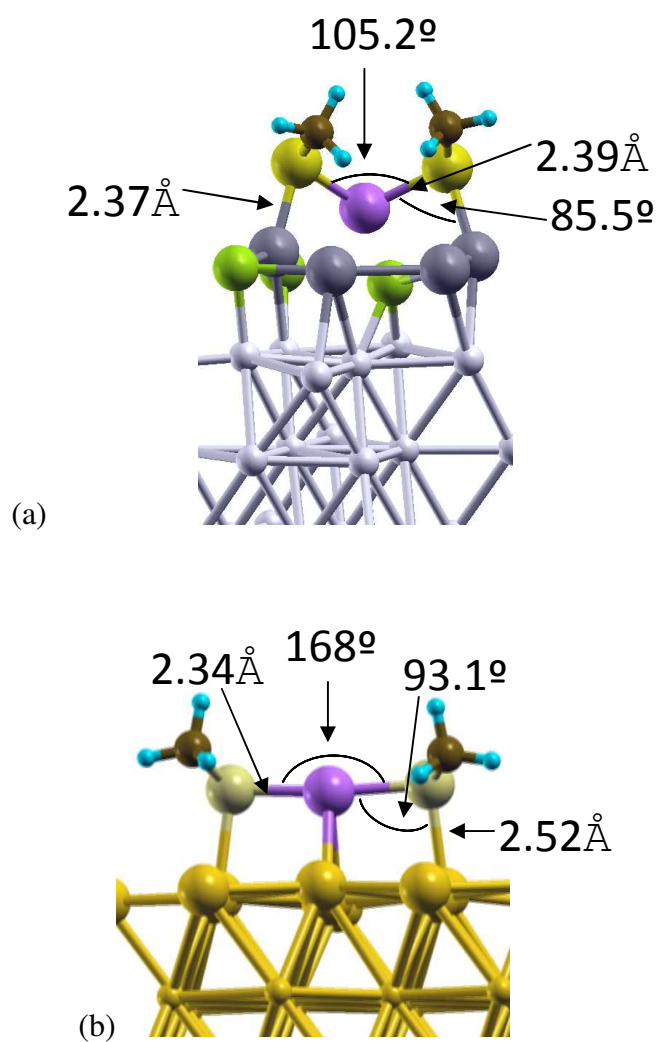
**Figure S5.** (a) Optimized structural parameters of model **4**. S: green, S in MT: yellow, C: brown, H: cyan, Pd adatom: violet, Pd top layer: dark grey, Pd second and deeper layers: light grey. (b) Optimized structural parameters for the Au adatom model described in References 6-7 in the text.

S in MT: yellow, C: brown, H: cyan, Au adatom: violet, Au top layer, Au second and deeper layers: orange.



(a)



(b)
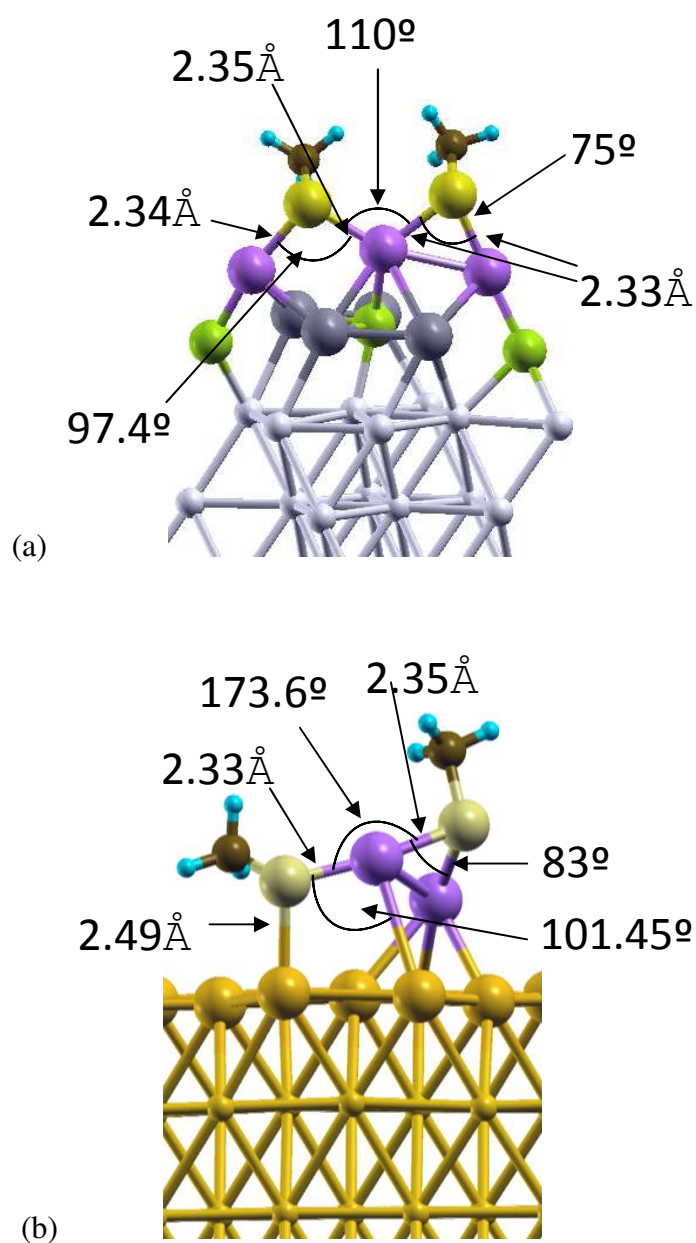
**Figure S6.** (a) Optimized structural parameters of model **5**. S: green, S in MT: yellow, C: brown, H: cyan, Pd adatom: violet, Pd toplayer: dark grey, Pd second and deeper layers: light grey. (b) Optimized structural parameters for the Au adatom model described in Reference 49 (see text). S

in MT: yellow, C: brown, H: cyan, Au adatom: violet, Au top layer, Au second and deeper layers: orange

## 6. PDOS of MT on Au(111)
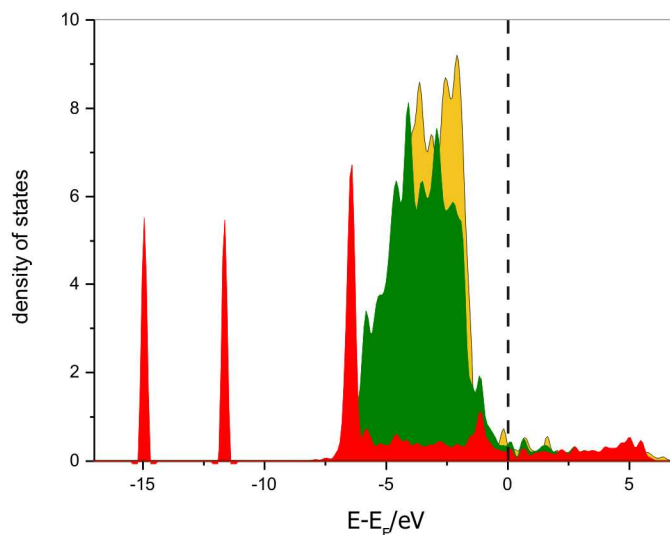


**Figure S7.** PDOS of √3x√3 R30° MT on Au(111). Yellow: topmost Au clean metal( d), green: topmost Au (d), red: MT ( s and p).

## References

(1)    Quayum, M.; Ye, S.; Uosaki, K. *J. Electroanal. Chem.* **2002**, *520*, 126-132.

(2)    Corthey, G.; Rubert, A. A.; Benitez, G. A.; Fonticelli, M. H.; Salvarezza, R. C. *J. Phys. Chem. C* **2009**, *113*, 6735-6742.

(3)    Kibler, L. A.; Kleinert, M.; Randler, R.; Kolb, D. M. *Surf. Sci.* **1999**, *443*, 19-30.

(4)    McQuarrie, D. A.; Simon, J. D. *Molecular thermodynamics*; University Science Books: Sausalito, CA, 1999.

(5)     Månsson, M.; Sunner, S. *Acta Chem. Scand.* **1962**, *16*, 1863-1869.

(6)     Finke, H. L.; Scott, D. W.; Gross, M. E.; Waddington, G.; Huffman, H. M. *J. Am. Chem. Soc.* **1952**, *74*, 2804-2806.